Asia-Pacific Journal of Atmospheric Sciences (2024) 60:479–493
https://doi.org/10.1007/s13143-024-00362-8

Online ISSN 1976-7951
Print ISSN 1976-7633

ORIGINAL ARTICLE

Characteristics of the Urban Heat Island in Dhaka, Bangladesh, and Its Interaction with Heat Waves

Abeda Tabassum[1] · Kyeongjoo Park[1] · Jaemyeong Mango Seo[1] · Ji-Young Han[2] · Jong-Jin Baik[1]

Received: 2 October 2023 / Revised: 11 March 2024 / Accepted: 19 March 2024 / Published online: 2 April 2024

Abstract

This study examines the characteristics of the urban heat island (UHI) in Dhaka, the densely populated capital city of Bangladesh under the influence of the South Asian monsoon, and its interaction with heat waves. For this, meteorological data at Dhaka (urban) and Madaripur (rural) stations and reanalysis data for the period of 1995–2019 are used for analysis. Here, the UHI intensity is defined as the urban-rural difference in 2-m temperature, and a heat wave is defined as the phenomenon which persists for two or more consecutive days with the daily maximum 2-m temperature exceeding its 90th percentile. The UHI intensity in Dhaka is in an increasing trend over the past 25 years (0.21 °C per decade). The average UHI intensity in Dhaka is 0.48 °C. The UHI is strongest in winter (0.95 °C) and weakest in the monsoon season (0.23 °C). In all seasons, the UHI is strongest at 2100 LST. The average daily maximum UHI intensity in Dhaka is 2.15 °C. Through the multiple linear regression analysis, the relative importance of previous-day daily maximum UHI intensity (PER), wind speed, relative humidity (RH), and cloud fraction which affect the daily maximum UHI intensity is examined. In the pre-monsoon season, RH is the most important variable followed by PER. In the monsoon season, RH is the predominantly important variable. In the post-monsoon season and winter, PER is the most important variable followed by RH. The occurrence frequency of heat waves in Dhaka shows a statistically significant increasing trend in the monsoon season (5.8 days per decade). It is found that heat waves in Bangladesh are associated with mid-to-upper tropospheric anticyclonic-flow and high-pressure anomalies in the pre-monsoon season and low-to-mid tropospheric anticyclonic-flow and high-pressure anomalies in the monsoon season. Under heat waves, the UHI intensity is synergistically intensified in both daytime and nighttime (nighttime only) in the pre-monsoon (monsoon) season. The decreases in relative humidity and cloud fraction are favorable for the synergistic UHI-heat wave interaction.

Keywords Dhaka · Urban heat island (UHI) · Heat wave · UHI-heat wave interaction · Monsoon

1 Introduction

The urban heat island (UHI) is a phenomenon that urban temperature is higher than surrounding rural temperature (Qian et al. 2022). The UHI has been extensively studied for numerous cities of the world (Oke et al. 2017). Many causative factors of the UHI are suggested, which include impervious surfaces, anthropogenic heat, and three-dimensional urban geometry that is subdivided into radiation trapping, additional heat stored in vertical walls, and wind speed reduction (Ryu and Baik 2012). The UHI intensity depends on the population, size, surface characteristics, background climate of a city, anthropogenic activities, topography, meteorological conditions, season, and the time of day (Kim and Baik 2002; Liu et al. 2007; Basara et al. 2008; Lee and Baik 2010; Jongtanom et al. 2011; Camilloni and Barrucand 2012; Cui and de Foy 2012; Schatz and Kucharik 2014; Zhao et al. 2014; Tzavali et al. 2015; Du et al. 2016; Wang et al. 2016; Kotharkar et al. 2019; Manoli et al. 2019; Zhang et al. 2022). For example, some cities experience stronger canopy-layer UHI in winter (Liu et al. 2007; Wang et al. 2016) while other cities exhibit stronger canopy-layer UHI in summer (Schatz and Kucharik 2014), and the canopy-layer UHI is typically stronger in the nighttime than in the daytime (Kim and Baik 2002; Jongtanom et al. 2011; Camilloni and Barrucand 2012).

✉ Jong-Jin Baik
jjbaik@snu.ac.kr

[1] School of Earth and Environmental Sciences, Seoul National University, Seoul 08826, South Korea

[2] Korea Institute of Atmospheric Prediction Systems, Seoul 07071, South Korea

The UHI can be altered under a heat wave, indicating the interaction between the UHI and heat wave (Li and Bou-Zeid 2013). The UHI-heat wave interaction has been investigated for many cities of the world (Kong et al. 2021). A number of studies have shown the synergistic UHI-heat wave interaction, that is, the enhancement of the UHI under heat waves (e.g., Founda and Santamouris 2017; Ortiz et al. 2018; Jiang et al. 2019; An et al. 2020). There are a few studies of the UHI-heat wave interaction for cities which are affected by the South Asian monsoon. Rizvi et al. (2019) showed that the maximum differences in canopy-layer UHI intensity between heat wave and non-heat wave days in Karachi, Pakistan are 3.0, 2.5, 2.8, and 2.7 °C when Ormara, Gwadar, Jiwani, and Pasni are considered as rural sites, respectively, indicating that the UHI-heat wave interaction in Karachi is synergistic. In contrast, Kumar and Mishra (2019) showed that under heat waves, 63% and 74% of the total urban areas in India exhibit declines in surface daytime and nighttime UHI intensities, respectively. It is known that the UHI-heat wave interaction varies depending on city size, background climate, and the large-scale (synoptic) characteristics of heat waves (Ramamurthy and Bou-Zeid 2017; Zhao et al. 2018; Park et al. 2023).

Bangladesh is one of the most densely populated countries in the world and has over 165 million inhabitants (BBS 2022). Many cities in the country have undergone rapid and unplanned urbanization. The characteristics of surface UHI in several cities of Bangladesh have been examined, including Chittagong (Ishtiaque et al. 2017; Roy et al. 2020; Gazi et al. 2021), Khulna (Islam and Islam 2013; Islam et al. 2019; Leya et al. 2022), Narayanganj (Rashid et al. 2022), and Dhaka (see the references below). The surface UHI in Dhaka, the capital city and the sixth most densely populated city in the world (Uddin et al. 2022), has been most extensively studied (Ahmed et al. 2013; Parvin and Abudu 2017; Dewan et al. 2021a, 2021b; Abrar et al. 2022; Rahman et al. 2022; Uddin et al. 2022). Uddin et al. (2022) analyzed the Moderate Resolution Imaging Spectroradiometer (MODIS)-based land surface temperature data for the period of 2001–2017 and showed that the daytime and nighttime surface UHI intensities in Dhaka significantly increased over years with their increasing rates of 0.03 °C per year and 0.023 °C per year, respectively. Using the MODIS data for the period of 2000–2019, Dewan et al. (2021a) examined surface UHI intensities in five major cities of Bangladesh. They identified population, lack of greenness, and anthropogenic forcing as the major factors that affect the surface UHI intensities. Dewan et al. (2021b) used the same data to further examine the diurnal and seasonal variations of surface UHI intensity. Using the air temperature data for Dhaka and its adjacent suburban area, Savar, Khatun et al. (2020) examined the canopy-layer UHI in Dhaka for the period of 1987–2016 and found the maximum UHI intensity of 3.5 °C.

While the previous studies of the UHI in Dhaka provide a comprehensive understanding of its characteristics, there are several areas of improvement that deserve further investigation. Firstly, all those studies except for Khatun et al. (2020) estimated surface UHI intensities using land surface temperatures derived from satellite data. For more complete understanding of the UHI in Dhaka, the canopy-layer UHI intensity also needs to be examined. Secondly, meteorological variables such as wind speed, relative humidity, and cloud cover affect UHI intensity (Kim and Baik 2002; Ganbat et al. 2013). However, none of the previous studies of the UHI in cities of Bangladesh examined the relative importance of meteorological variables that affect UHI intensity. Lastly, the UHI-heat wave interaction in Dhaka is not studied yet despite the awareness of worsening thermal comfort in Dhaka due to urbanization and global warming (Shourav et al. 2018; Imran et al. 2021). These three aspects motivate the present study.

In this study, using long-term meteorological data and reanalysis data, we examine the temporal characteristics of the UHI in Dhaka and its interaction with heat waves. Section 2 describes the data and methods. In Section 3, the analysis results are presented and discussed. Section 4 gives a summary and conclusions.

2 Data and Methods

To examine the characteristics of the UHI in Dhaka, 25-year data at two meteorological stations from 1995 to 2019 are obtained from the Bangladesh Meteorological Department (BMD). The data include the 2-m temperature, 10-m wind speed, relative humidity, and cloud fraction (in octa scale) in 3-h intervals as well as the daily precipitation amount, the daily maximum 2-m temperature, and the daily minimum 2-m temperature. Dhaka station is selected as the urban station, and Madaripur station located on the south-southwest of Dhaka station is selected as the rural station (Fig. 1). Madaripur station is located in a highly vegetated area and experiences the same background climate as Dhaka station (Beck et al. 2018). The urban land use fraction within a 1-km^2 circle centered on Dhaka station (Madaripur station) in 2019, estimated using the Landsat 8 Operational Land Imager data (Roy et al. 2014; Ouchra et al. 2023), is 48% (6%). The urban land use fraction around Madaripur station does not notably change during the study period. In this study, the UHI intensity is defined as the difference in 2-m temperature between Dhaka and Madaripur stations and the daily maximum UHI intensity is defined as the largest difference in 2-m temperature between the two stations for each day. Excluding 2927 missing data (2% of total), 143169 measurement data are used to calculate the UHI intensity. To analyze the seasonal variations of the UHI intensity,

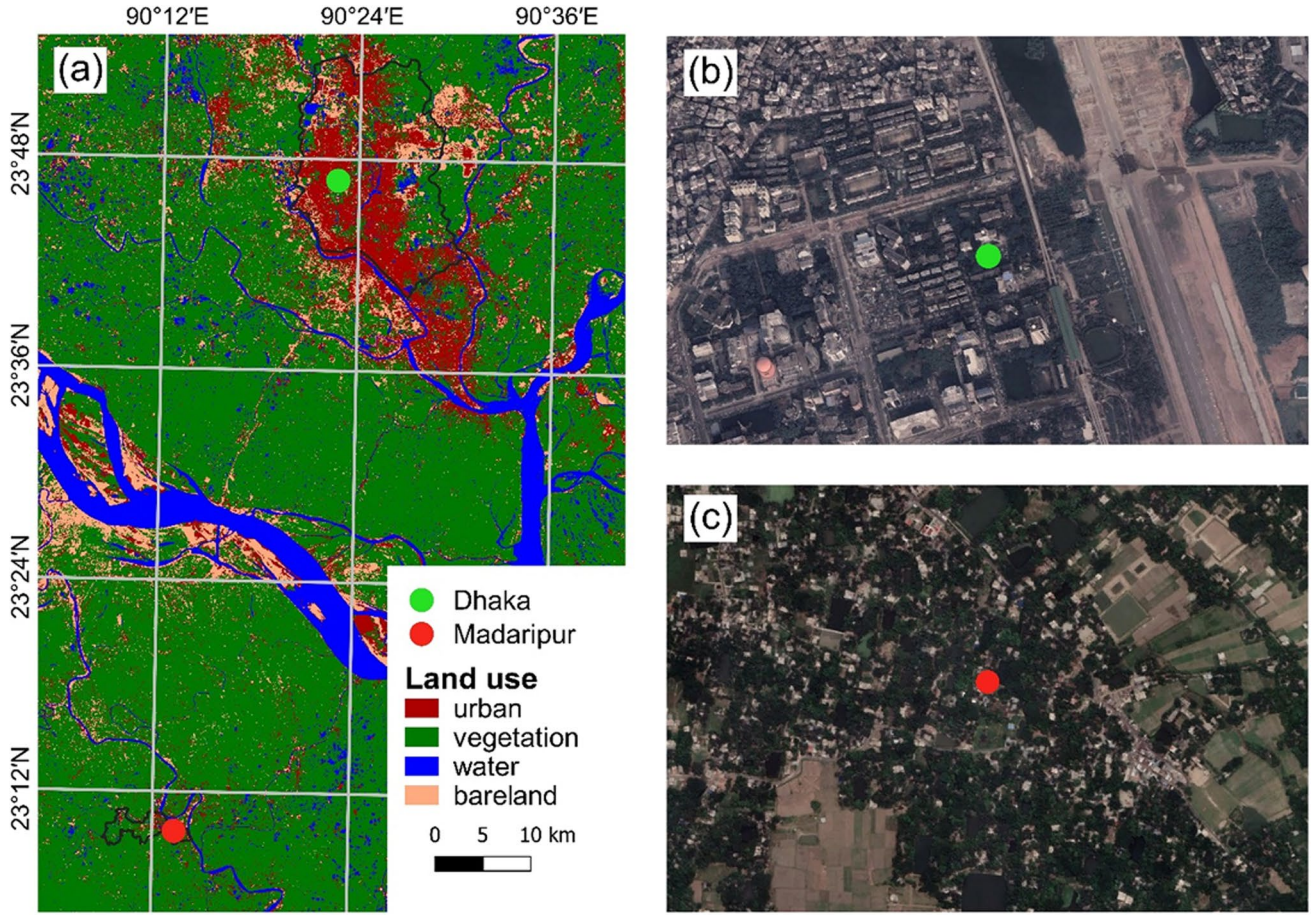

Fig. 1 (**a**) Land use map of Dhaka and Madaripur (contoured by black solid lines) and their neighboring regions in 2019 based on the Landsat 8 Operational Land Imager data. The locations of Dhaka and Madaripur stations are marked in green and red circles, respectively. Satellite images around (**b**) Dhaka station and (**c**) Madaripur station in 2023 (Google Earth image)

the entire year is divided into four seasons: pre-monsoon season (March, April, and May), monsoon season (June, July, August, and September), post-monsoon season (October and November), and winter (December, January, and February) (Ahmed et al. 2020). For the study period, the annual precipitation amount averaged over the two stations is 1942 mm, and the percentage of precipitation amount in each season to the annual precipitation amount is 21% in the pre-monsoon season, 67% in the monsoon season, 10% in the post-monsoon season, and 2% in winter.

To examine the relative importance of meteorological variables that affect the daily maximum UHI intensity, the wind speed, relative humidity, and cloud fraction data at Dhaka station are used to perform a multiple linear regression analysis. Here, the relative importance means which independent variable is relatively more important one for the dependent variable. Following Kim and Baik (2002), the dependent variable is the daily maximum UHI intensity and the independent variables are the daily maximum UHI intensity for the previous day, wind speed, relative humidity, and cloud fraction. For the wind speed, relative humidity, and cloud fraction, the values at the time of the daily maximum UHI intensity are used. Before the multiple linear regression analysis is performed, the standardization for data of each variable is made by subtracting their mean and then dividing by their standard deviation. This allows a direct comparison of regression coefficients of different variables and thus an examination of their relative importance. In classifying daytime and nighttime, 0900, 1200, 1500, and 1800 local standard time (LST) are considered as daytime and 2100, 0000, 0300, and 0600 LST are considered as nighttime.

In Bangladesh, the occurrence of heat waves is mainly concentrated in May and June which belong to the pre-monsoon and monsoon seasons, respectively (Nissan et al. 2017). So, the UHI-heat wave interaction in those seasons is examined. In this study, the threshold air temperature in defining a heat wave is based on the TX90p criterion (Perkins 2015) which is the 90th percentile of daily maximum temperatures. This criterion has been widely used in defining a heat wave (Panda et al. 2017; Erlat et al. 2021; Engdaw et al. 2022). We adopt

the threshold duration of two days, so that in this study, a heat wave is defined as the phenomenon which persist for two or more consecutive days with the daily maximum 2-m temperature averaged for the two stations exceeding the 90th percentile for each season. The 90th percentile of the daily maximum 2-m temperature is 36.2 °C in the pre-monsoon season and 34.7 °C in the monsoon season. 172 days and 225 days are classified as heat wave days in the pre-monsoon season and monsoon season, respectively. The remaining 2128 and 2825 days are classified as non-heat wave days in the pre-monsoon season and monsoon season, respectively. To analyze the UHI-heat wave interaction, the statistical distributions and diurnal variations of the UHI intensities under heat wave and non-heat wave days in each season are compared. The synergistic UHI-heat wave interaction is referred to as the increase in UHI intensity during heat wave days compared to non-heat wave days (Li and Bou-Zeid 2013), since the increase in UHI intensity during heat waves indicates both the enhancement of the UHI due to heat waves and the enhancement of heat waves in urban areas due to the UHI. The daily maximum temperature, daily minimum temperature, and daytime/nighttime wind speed, relative humidity, and cloud fraction under heat wave and non-heat wave days in each season are also compared to examine how meteorological conditions under heat waves differ from those under non-heat waves. For this, each meteorological variable is averaged over Dhaka and Madaripur stations to consider background meteorological conditions that affect both urban and rural areas. In comparing UHI intensity and meteorological conditions under heat waves with those under non-heat waves, the data with daily precipitation amount at the urban or rural station being larger than 0.1 mm are excluded from the analysis (Jiang et al. 2019; Park et al. 2023).

For each of the pre-monsoon and monsoon seasons, how synoptic patterns under heat waves differ from the mean climatology is investigated. For this, the European Centre for Medium-range Weather Forecasts (ECMWF) reanalysis 5 (ERA5) data (Hersbach et al. 2020) are used. The data have $0.25° \times 0.25°$ horizontal resolution and 1-h temporal resolution. The fields of 200-, 500-, and 850-hPa geopotential heights and horizontal wind velocities, vertical wind velocities, and 850-hPa specific humidity are analyzed. These levels are typically considered to analyze synoptic patterns associated with heat waves (Zhang et al. 2020; Cao et al. 2022; Cha et al. 2022; Jiang et al. 2023).

3 Results and Discussion

3.1 Yearly, Seasonal, and Diurnal Variations of the UHI

In this subsection, the yearly, seasonal, and diurnal variations of UHI intensity in Dhaka are examined. Figure 2a shows the yearly variations of annually averaged temperatures in Dhaka and Madaripur for the 25-year period. The yearly trends are calculated through the linear regression analysis. The statistical significances of yearly trends are determined at the 95% confidence level. Both Dhaka and Madaripur exhibit increasing trends in annually averaged temperature. The increasing rate in Dhaka (0.25 °C per decade, statistically significant) is five times larger than that in Madaripur (0.05 °C per decade, statistically insignificant). The annually averaged temperature is consistently higher in Dhaka than in Madaripur. The UHI intensity tends to increase over years, with its increasing rate of 0.21 °C per decade (Fig. 2b). This increasing rate is comparable to those in other cities [e.g., 0.31 °C per decade in Beijing, China (Lin and Yu 2005), 0.22 °C per decade in Athens, Greece (Founda et al. 2015), and 0.24 °C per decade in Lanzhou, China (Li et al. 2018)]. The UHI intensity averaged over the study period is 0.48 °C. This is much weaker than the UHI intensities in other cities of the world [e.g., 2.1 °C in

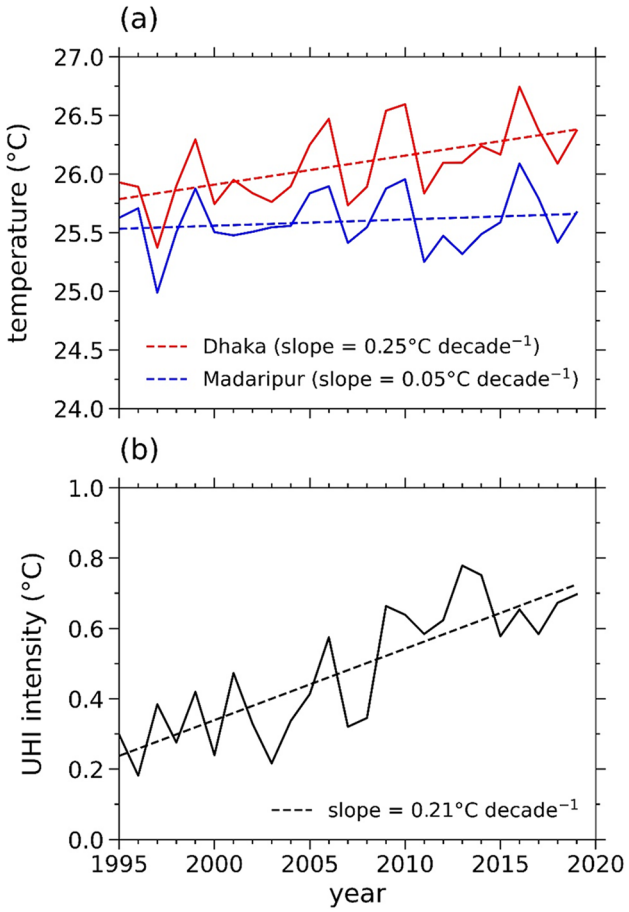

Fig. 2 Yearly variations of (**a**) annually averaged temperatures in Dhaka (red) and Madaripur (blue) and their linear trends and (**b**) yearly variation of annually averaged UHI intensity and its linear trend

Minneapolis-St. Paul, U.S.A. (Todhunter 1996), 2.2 °C in Seoul, South Korea (Kim and Baik 2005), 1.6 °C in Ulaanbaatar, Mongolia (Ganbat et al. 2013), and 0.8 °C in Bangkok, Thailand (Arifwidodo and Tanaka 2015)]. One plausible reason for the weaker UHI intensity in Dhaka is that the Dhaka station is located in a partially vegetated area (26% within the surrounding 1-km^2 circle centered on the Dhaka station), which could mitigate the difference in 2-m temperature between the two stations. Khatun et al. (2020) found a decreasing trend of UHI intensity in Dhaka during 1987–2016 when Savar station, which is located in a suburban area, was selected and concluded that the decreasing trend of the UHI intensity is attributed to increasing temperature in Savar due to industrialization. Another plausible reason for the weaker UHI intensity in Dhaka is that Dhaka and its surrounding areas are affected by the South Asian monsoon, which experience frequent and heavy rainfalls in the monsoon season. Precipitation weakens the UHI (Lee and Baik 2010) or makes the UHI disappear.

The seasonally averaged UHI intensity in Dhaka is presented in Fig. 3. The UHI is strongest in winter (0.95 °C) and weakest in the monsoon season (0.23 °C). The relatively very small precipitation amount in winter may contribute to the strongest UHI. The pre-monsoon season exhibits the second strongest UHI (0.42 °C). Santamouris (2015) reviewed 88 articles on UHI intensities in 101 cities worldwide and found that the UHI intensity is strongest in dry season for cities with climate characterized by dry and humid periods. The UHI intensity in Dhaka calculated in this study is, however, weaker than those in other cities with this climate [e.g., 1.65 °C in Beijing (Yang et al. 2013), 3.9 °C in Presidente Prudente, Brazil (Amorim 2020), and 2.38 °C in Delhi, India (Kumar et al. 2023)].

Figure 4 shows the diurnal variations of annually and seasonally averaged UHI intensities. The diurnal variation of annually averaged UHI intensity exhibits its maximum at 2100 LST (1.00 °C) and its minimum at 1200 LST (−0.08 °C). A similar pattern is observed in many cities around the world (e.g., Basara et al. 2008; Kim et al. 2017; Vogel and Afshari 2020). At most of hours, the UHI is strongest in winter and weakest in the monsoon season. At 2100 LST, the UHI is strongest in all seasons, being 3.3 times larger in winter (1.70 °C) than in the monsoon season (0.51 °C). The diurnal amplitude of UHI intensity in winter is larger compared to those in other seasons. This feature also appears in Ulaanbaatar (Ganbat et al. 2013). In contrast, in Buenos Aires, Argentina, the largest diurnal amplitude of UHI intensity appears in summer (Camilloni and Barrucand 2012). In all seasons, the weak urban cool island is observed. The urban cool island is most prominent in the pre-monsoon season, with its maximum intensity of 0.22 °C at 1200 LST, but weaker than the urban cool islands observed in several tropical cities located in Southeast Asia (e.g., Chow and Roth 2006; Harun et al. 2020). The urban cool island is primarily attributed to the shading due to the urban canopy, the relatively strong urban planetary boundary layer mixing, and the attenuation of solar radiation by urban air pollutants (Chow and Roth 2006; Memon et al. 2009; Theeuwes et al. 2015), and its causes for Dhaka deserve

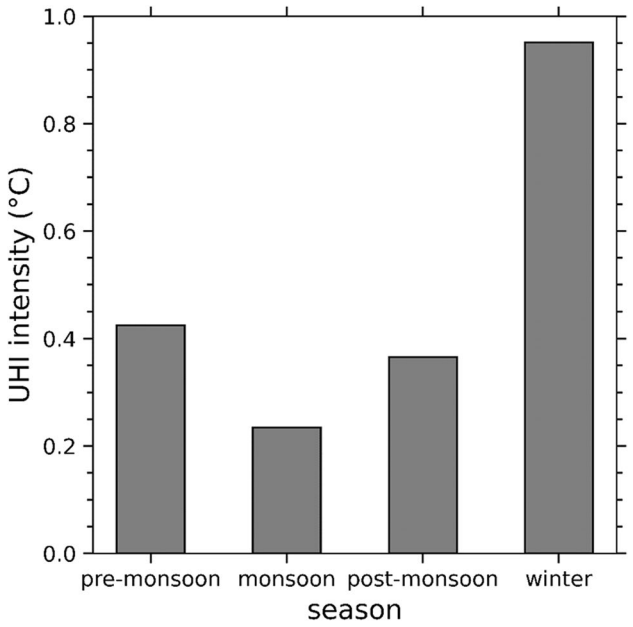

Fig. 3 Seasonal variation of UHI intensity

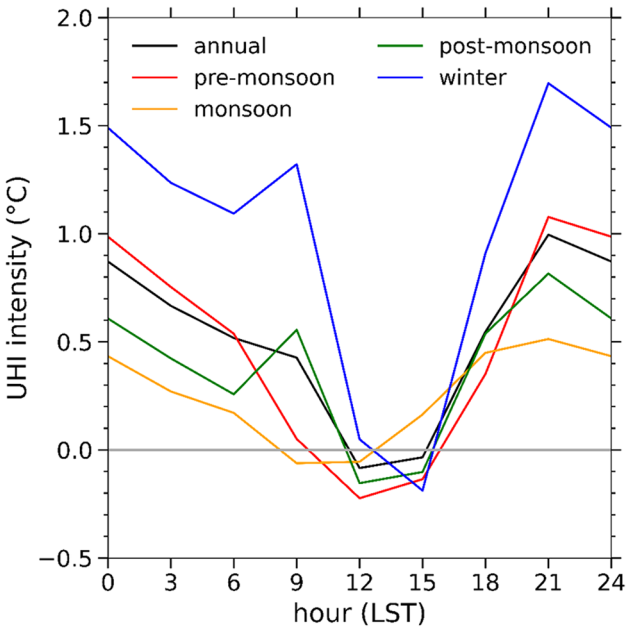

Fig. 4 Diurnal variation of annually averaged UHI intensity (black) and those of seasonally averaged UHI intensities (colored). The horizontal gray line indicates zero

further investigation. It is interesting to observe that a secondary peak in the diurnal variation of UHI intensity appears at 0900 LST in the post-monsoon season (0.56 °C) and winter (1.32 °C). The anthropogenic heat associated with increased transportation could be a possible contributing factor to these pronounced UHI intensities in the morning (Theeuwes et al. 2015; Wang et al. 2023), but further investigation with high-resolution anthropogenic heat emission data for Dhaka is needed to quantify this effect on the UHI.

3.2 Daily Maximum UHI Intensity

The characteristics of daily maximum UHI intensity in Dhaka and its association with meteorological variables are examined in this subsection. Figure 5 shows the yearly variations of annually and seasonally averaged daily maximum UHI intensities. The annually averaged daily maximum UHI intensity exhibits an increasing trend over the 1995–2019 period (0.24 °C per decade). The increasing trend is most pronounced in winter (0.58 °C per decade) followed by the post-monsoon season (0.41 °C per decade) and pre-monsoon season (0.11 °C per decade). There is no increasing trend in the monsoon season (0.00ºC per decade). In contrast with Dhaka, some other cities exhibit more pronounced increasing trends of UHI intensity in summer than in winter (e.g., Wang et al. 2016; Varentsov et al. 2020; Yao et al. 2021). For instance, Wang et al. (2016) showed that the increasing rate of the daily maximum UHI intensity in Hong Kong, China is larger in summer (0.14ºC per decade) than in winter (0.09ºC per decade). The daily maximum UHI intensity averaged over the study period is 2.15 °C, which is 4.5 times larger than the UHI intensity averaged over the same period. Over the study period, the seasonally averaged daily maximum UHI intensity is strongest in winter (2.79 °C) and weakest in the monsoon season (1.76 °C).

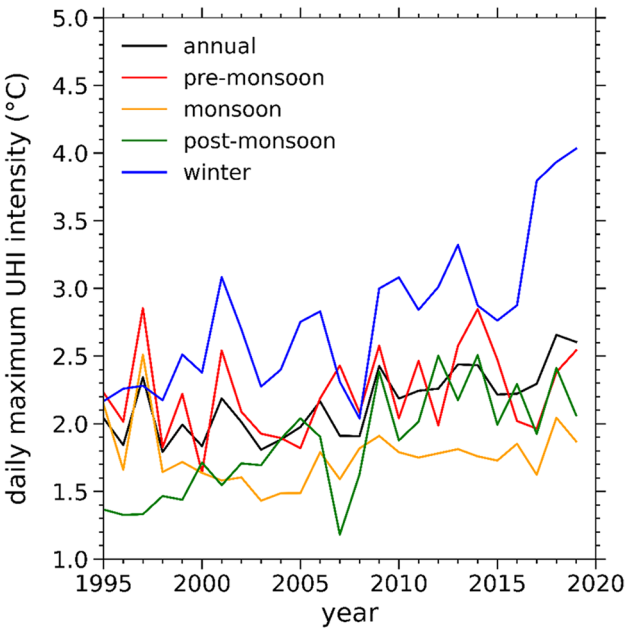

Fig. 5 Yearly variation of annually averaged daily maximum UHI intensity (black) and those of seasonally averaged daily maximum UHI intensities (colored)

The occurrence frequencies of daily maximum UHI intensity at different times of day for the whole year and each season are presented in Fig. 6. For the whole year (Fig. 6a), the occurrence frequency peaks at 2100 LST (0.19). Interestingly, there is a clear peak in the occurrence frequency at 0900 LST. The difference between the daytime and nighttime averaged occurrence frequencies is not large (0.01). This is in contrast with previous studies which typically show a pronounced higher occurrence frequency of daily maximum UHI intensity in the nighttime (e.g., Ganbat et al. 2013). In the pre-monsoon season (Fig. 6b), there are a distinct peak at 2100 LST (0.27) and a less pronounced secondary peak at 0600 LST. The monsoon season has, among the four seasons, only one peak in the occurrence frequency which occurs at 1500 LST (Fig. 6c). In the post-monsoon season (Fig. 6d), the highest peak occurs at 0900 LST and the second highest peak occurs at 1800 LST. In winter (Fig. 6e), there are the highest peak at 2100 LST and the second highest peak at 0900 LST. The daily maximum UHI intensity occurs more frequently in the daytime than in the nighttime in the monsoon and post-monsoon seasons, while the opposite is true for the pre-monsoon season and winter. These higher nighttime occurrence frequencies of the daily maximum UHI intensity in the pre-monsoon season and winter can be attributed to the notably strong nighttime UHI intensities in these seasons (Fig. 4).

Next, the relative importance of the meteorological variables that affect the daily maximum UHI intensity is investigated. Table 1 lists the standardized regression coefficients of daily maximum UHI intensity for the previous day (PER), wind speed (WS), relative humidity (RH), and cloud fraction (CF) obtained by the multiple linear regression analysis using all and each season data. For all data, the variance explained by the multiple linear regression model (R^2) is 20.5%. The standardized regression coefficient of RH is −0.31. RH is, among the four variables, the most important variable that affects the daily maximum UHI intensity. RH is negatively correlated with the daily maximum UHI intensity, that is, higher (lower) RH acts to weaken (strengthen) the UHI. The high relative humidity reduces the warming/cooling rate of air by increasing its thermal admittance, being able to decrease the UHI intensity (Schatz and Kucharik 2014; Thomas et al. 2014). The standardized regression coefficient of PER is 0.23. PER is the second most important variable and is positively correlated with the daily maximum UHI intensity. PER indicates the persistence

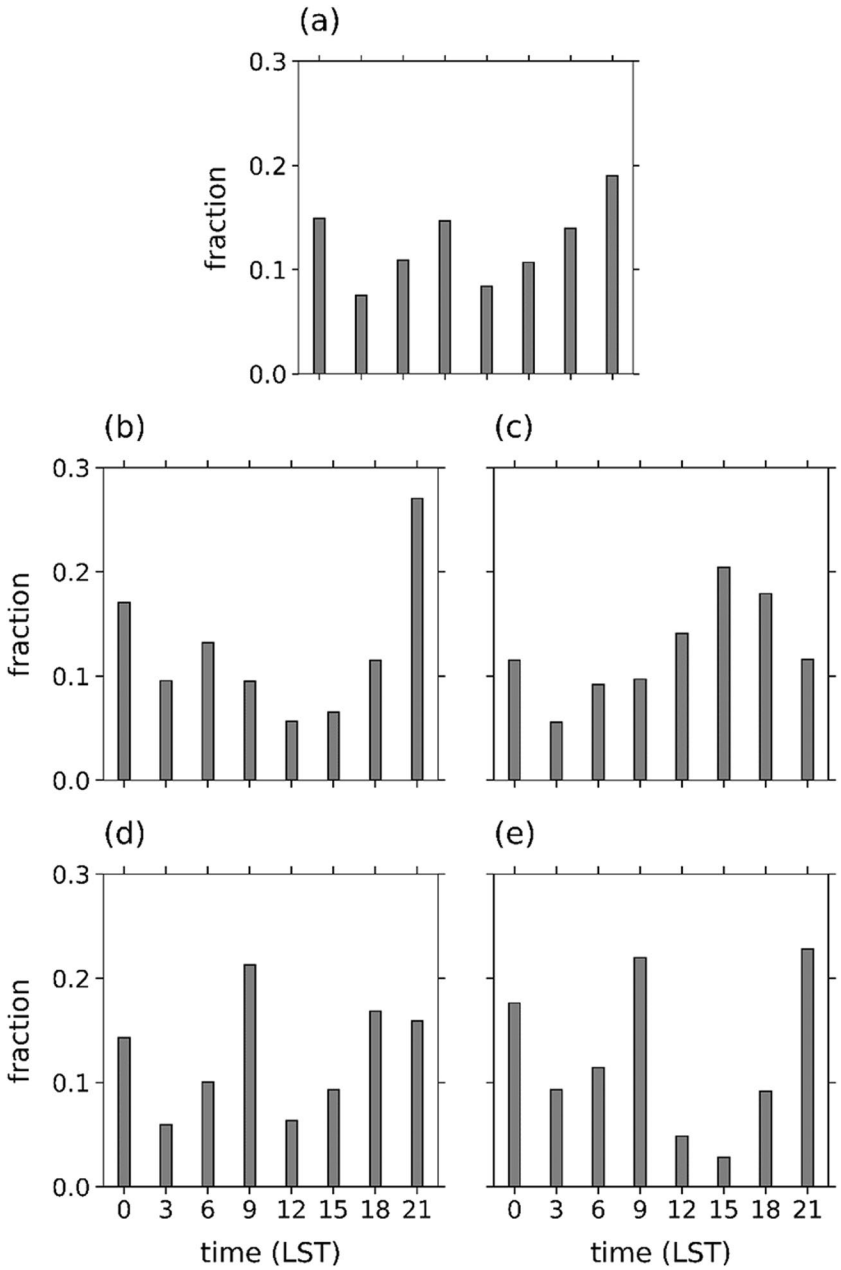

Fig. 6 Occurrence frequency of daily maximum UHI intensity at different times of day for (**a**) the whole year, (**b**) pre-monsoon, (**c**) monsoon, (**d**) post-monsoon, and (**e**) winter

Table 1 Standardized regression coefficients of daily maximum UHI intensity for the previous day (PER), wind speed (WS), relative humidity (RH), and cloud fraction (CF) for all data and in each season. R^2 denotes the total variance explained by the multiple linear regression model, and N is the sample size. The asterisk indicates statistical significance at the 95% confidence level

	All	Pre-monsoon	Monsoon	Post-monsoon	Winter
PER	0.23*	0.21*	0.05*	0.31*	0.38*
WS	0.02*	–0.01	0.05*	0.00	0.02
RH	–0.31*	–0.38*	–0.37*	–0.25*	–0.24*
CF	–0.09*	0.02	0.07*	–0.05	–0.11*
R^2 (%)	20.5	21.7	13.9	18.0	25.0
N	9042	2295	3041	1521	2185

of the UHI. CF is negatively correlated with the daily maximum UHI intensity (its regression coefficient is −0.09). The high cloud fraction hinders the receipt of shortwave radiation, being able to decrease the UHI intensity (Morris et al. 2001; He 2018). WS is, unexpectedly, positively correlated with the daily maximum UHI intensity, but the magnitude of its regression coefficient is very small (0.02) compared to those of the other three variables.

In seasonal classification, R^2 is largest in winter (25.0%) followed by the pre-monsoon (21.7%), post-monsoon (18.0%), and monsoon (13.9%) seasons. In the pre-monsoon season, RH is the most important variable (regression coefficient of −0.38) followed by PER (0.21), CF (0.02), and WS

(−0.01). In the monsoon season, RH is the most important variable (−0.37) and CF is the second most important variable (0.07). It is notable that the regression coefficient of PER in the monsoon season (0.05) is much smaller compared to those in other seasons. In the post-monsoon season, PER (0.31) is the most important variable followed by RH (−0.25), CF (−0.05), and WS (0.00). In winter, the relative importance of the four variables and the sign of the regression coefficient for each variable are the same as those in the post-monsoon season.

The four variables (PER, WS, RH, and CF) were previously used to study their association with the daily maximum UHI intensity through the multiple linear regression analysis for Seoul (Kim and Baik 2002) and Ulaanbaatar (Ganbat et al. 2013). Therefore, direct comparisons of total variances explained by the multiple linear regression models and standardized regression coefficients for the three cities are possible. For all data, R^2 for Dhaka (20.5%) is smaller than R^2 for Seoul (46.1%) and Ulaanbaatar (49.8%). PER is the most important variable for Seoul and Ulaanbaatar, while it is the second most important variable for Dhaka. A notable difference is found in the relative importance of RH. RH is the least important variable for Seoul and Ulaanbaatar, while it is the most important variable for Dhaka. The importance of relative humidity on the UHI intensity was also reported in several other cities that experience tropical climate like Dhaka (e.g., Ramakreshnan et al. 2019; Kamma et al. 2020). According to the Köppen-Geiger climate classification (Kottek et al. 2006; Peel et al. 2007; Beck et al. 2018), Dhaka, Seoul, and Ulaanbaatar belong to tropical savannah climate (Aw), humid continental climate (Dwa), and cold semi-arid climate (BSk), respectively. Madaripur has the same background climate as Dhaka. We speculate that background climates are to some or a great extent responsible for the differences in R^2 and the relative importance of the four variables between the three cities.

The total data are classified into daytime and nighttime data, and the multiple linear regression analysis is performed for each data (not shown). The variance explained by the regression model for the daytime maximum UHI intensity is 8.9%, and that for the nighttime maximum UHI intensity is 40.2%. For Seoul, the variance explained by the regression model for the nighttime maximum UHI intensity is also larger than that for the daytime maximum UHI intensity (Kim and Baik 2002). For Ulaanbaatar, the opposite is reported (Ganbat et al. 2013). The ratio of the variance explained by the regression model for the nighttime maximum UHI intensity to that for the daytime maximum UHI intensity is 4.5 for Dhaka, 1.6 for Seoul, and 0.8 for Ulaanbaatar, showing large differences. We also speculate that background climates are to some or a great extent responsible for these differences.

3.3 Interaction between the UHI and Heat Waves

This subsection examines the interaction of the UHI in Dhaka with heat waves. Figure 7 shows the yearly variations of occurrence frequencies of heat waves in the pre-monsoon and monsoon seasons. The long-term trend of occurrence frequency of heat waves in the pre-monsoon season (HW_{pre}) is in contrast with that in the monsoon season (HW_{mon}). The HW_{pre} occurrence frequency exhibits a statistically insignificant decreasing trend (−2.5 days per decade), while the HW_{mon} occurrence frequency exhibits a statistically significant increasing trend (5.8 days per decade). The increase in HW_{mon} occurrence frequency is more pronounced in the recent decade with its increasing rate of 12.2 days per decade for the period of 2008–2019.

To investigate how synoptic features under heat waves differ from mean climatology in each season, composite fields of geopotential height anomalies and horizontal wind-anomaly vectors at the 200-, 500-, and 850-hPa levels are plotted (Fig. 8). Here, the anomaly at each grid point is a deviation from the value averaged over the days that include both heat wave days and non-heat wave days. Under HW_{pre}, Bangladesh is under the influence of anticyclonic-flow and high-pressure anomalies at the 200-hPa level whose center is located north of Bangladesh (Fig. 8a). This is consistent with the result of Zahid and Rasul (2012) that in the pre-monsoon season, the Tibetan high is crucial for the development of heat waves in the South Asian region. At the 500-hPa level, anticyclonic-flow and high-pressure anomalies are also seen (Fig. 8b). At the 850-hPa level, weak anticyclonic-flow anomalies appear in Bangladesh but the geopotential height anomalies are negative (Fig. 8c). The 850-hPa vertical velocity averaged over a small area (23.25–23.75°N, 90.25–90.75°E) which includes Dhaka and Madaripur is −0.06 Pa s^{-1}. There is subsidence in the mid-to-upper troposphere, with vertical velocities of 0.04 Pa s^{-1} at the 500-hPa level and 0.01 Pa s^{-1} at the 200-hPa level. Under HW_{mon}, high-pressure anomalies are prominent in the Indian region at the 850- and 500-hPa levels and the eastern edges of these high-pressure anomalies cover Bangladesh (Figs. 8e and f). At the 200-hPa level, the high-pressure anomalies in the lower-to-mid troposphere are not seen and southwesterly wind anomalies prevail (Fig. 8d). The rising motion is highly suppressed under HW_{mon}. The vertical velocity anomalies under HW_{mon} are 0.04, 0.05, and 0.03 Pa s^{-1} at the 200-, 500-, and 850-hPa levels, respectively. The anticyclonic-flow anomalies in the lower troposphere counteract the prevailing monsoonal southerly winds, hindering the moisture transport from the Bay of Bengal. The 850-hPa specific humidity decreases in the Bay of Bengal and the study area under both HW_{pre} and HW_{mon} (not shown). In summary, HW_{pre} is associated with anticyclonic-flow and high-pressure anomalies in the mid-to-upper troposphere, while HW_{mon} is associated

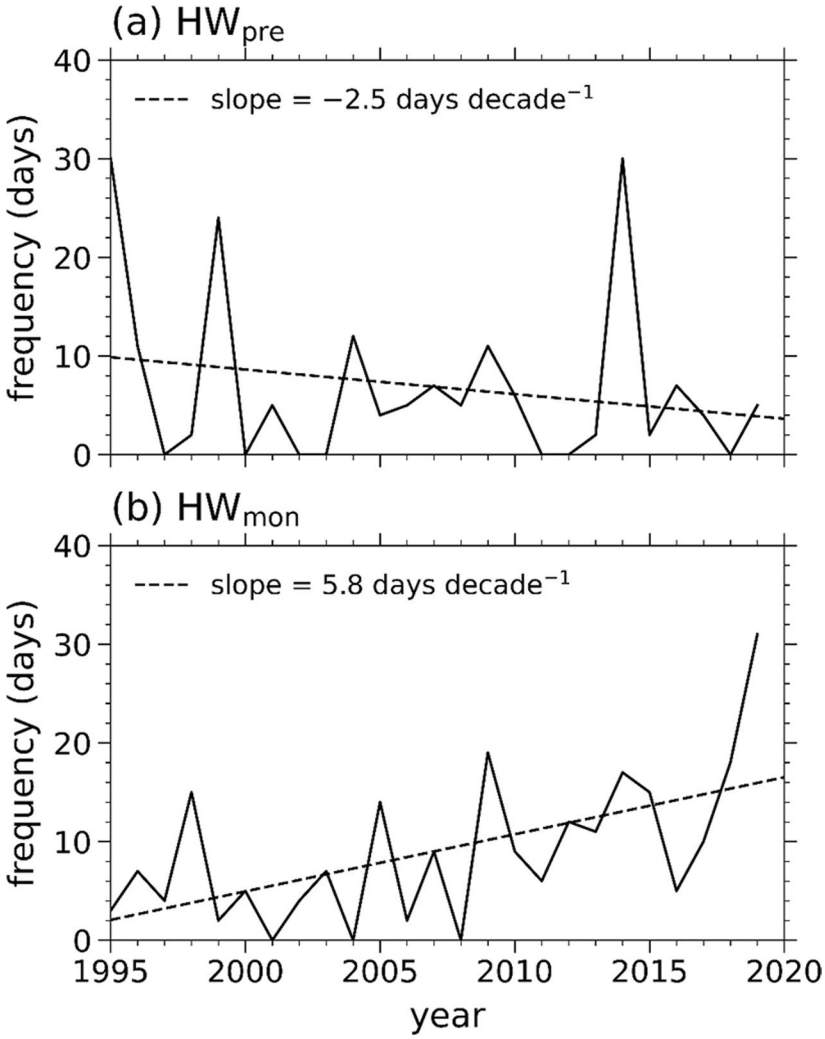

Fig. 7 Yearly variations of occurrence frequencies of heat waves in the (**a**) pre-monsoon and (**b**) monsoon seasons. The dashed lines are their linear trends

with anticyclonic-flow and high-pressure anomalies in the lower-to-mid troposphere.

Table 2 lists daily maximum/minimum 2-m temperature (T_{max}/T_{min}) and daytime/nighttime 10-m wind speed, relative humidity, and cloud fraction under HW_{pre}, $nonHW_{pre}$ (non-heat waves in the pre-monsoon season), HW_{mon}, and $nonHW_{mon}$ (non-heat waves in the monsoon season) along with their respective differences in each season. Under HW_{pre}, T_{max} and T_{min} increase by 3.4 °C and 2.8 °C, respectively. The diurnal temperature range increases by 0.6 °C. The daytime and nighttime 10-m wind speeds increase, while both daytime and nighttime relative humidities and cloud fractions decrease. Under HW_{mon}, T_{max} and T_{min} increase by 2.2 °C and 0.7 °C, respectively, with 1.5 °C increase in the diurnal temperature range. The daytime and nighttime relative humidities and cloud fractions decrease. The daytime (also nighttime) relative humidity is higher under HW_{mon} than under HW_{pre}. This is also true for non-heat waves. The difference in daytime relative humidity between heat wave and non-heat wave days is much larger in the monsoon season than in the pre-monsoon season.

Figures 9a, b, and c show the box plots of daytime and nighttime UHI intensities and the diurnal variations of UHI intensities under HW_{pre} and $nonHW_{pre}$. Under HW_{pre}, the statistical distributions (mean, median, upper and lower quartiles, and 90th and 10th percentiles) of both daytime and nighttime UHI intensities exhibit increasing shifts (Figs. 9a and b). The mean daytime and nighttime UHI intensities are stronger under HW_{pre} (0.45 °C and 1.34 °C, respectively) than under $nonHW_{pre}$ (0.11 °C and 1.07 °C, respectively). Note that the mean daytime and nighttime urban (rural) 2-m temperatures are higher by 3.46 °C (3.12 °C) and 2.90 °C (2.52 °C) under HW_{pre} than under $nonHW_{pre}$, respectively. Thus, the increase in UHI intensity under heat waves represents an additional warming effect in the urban area in addition to background heat waves and UHI effects. This effect further intensifies heat waves in the urban area, which is called the synergistic UHI-heat wave interaction (Li and Bou-Zeid 2013). The 10th percentiles of daytime and nighttime UHI intensities under $nonHW_{pre}$ are −1.05 °C and −0.05 °C, both exhibiting urban cool islands. The 10th

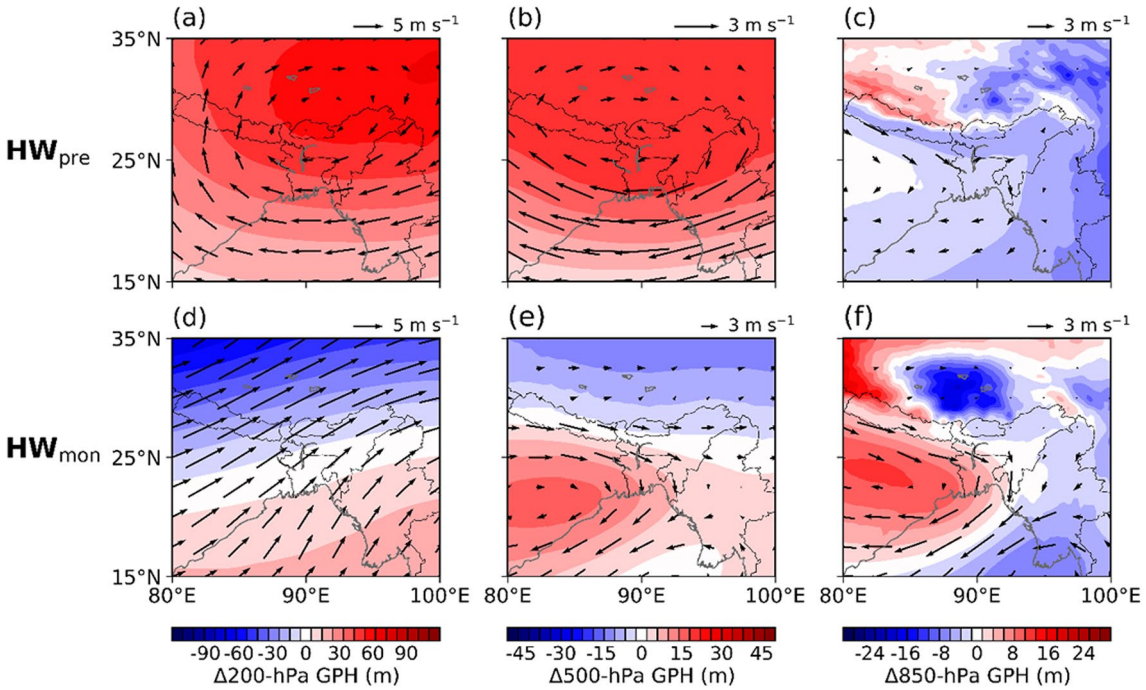

Fig. 8 Composite fields of geopotential height anomalies and horizontal wind-anomaly vectors at the (**a**) 200-, (**b**) 500-, and (**c**) 850-hPa levels under heat waves in the pre-monsoon season. (**d**, **e**, **f**) Same as (**a**, **b**, **c**) except for the monsoon season

Table 2 Daily maximum 2-m temperature (T_{max}), daily minimum 2-m temperature (T_{min}), and daytime/nighttime 10-m wind speed, relative humidity, and cloud fraction averaged over heat wave days and non-heat wave days along with their respective differences in the pre-monsoon and monsoon seasons. The value of each meteorological variable is the average of the values at Dhaka and Madaripur stations. The asterisk indicates statistical significance at the 95% confidence level

	T_{max}/T_{min} (°C)	daytime/nighttime wind speed (m s^{-1})	daytime/nighttime relative humidity (%)	daytime/nighttime cloud fraction
HW_{pre}	37.1/26.0	1.12/0.72	53.9/80.7	2.5/2.0
$nonHW_{pre}$	33.6/23.2	0.96/0.54	57.7/82.4	3.2/2.3
$HW_{pre} - nonHW_{pre}$	3.4*/2.8*	0.16*/0.17*	–3.8*/–1.7*	–0.7*/–0.3*
HW_{mon}	35.5/27.7	0.69/0.41	67.5/86.9	4.6/3.9
$nonHW_{mon}$	33.4/27.0	0.71/0.39	74.2/88.6	5.8/5.2
$HW_{mon} - nonHW_{mon}$	2.2*/0.7*	–0.02/0.03	–6.6*/–1.8*	–1.2*/–1.1*

percentiles of daytime and nighttime UHI intensities under HW_{pre} are −0.33 °C and 0.47 °C, showing considerable increases by 0.72 °C and 0.52 °C. Meanwhile, the 90th percentiles of daytime and nighttime UHI intensities under HW_{pre} (1.30 °C and 2.35 °C) show relatively slight increases by 0.10 °C and 0.07 °C. Thus, the degree of the synergistic UHI-heat wave interaction in the pre-monsoon season is larger in the low percentiles of daytime and nighttime UHI intensities than in the high percentiles of daytime and nighttime UHI intensities.

The diurnal variations of UHI intensities under HW_{pre} and $nonHW_{pre}$ also indicate the synergistic UHI-heat wave interaction throughout the day except for 0900 LST when the UHI intensity is very slightly larger under $nonHW_{pre}$ than under HW_{pre} (Fig. 9c). Despite the most pronounced increase in UHI intensity at 2100 LST under HW_{pre} by 0.50 °C, the synergistic UHI-heat wave interaction is considerably strong in the daytime at 1200, 1500, and 1800 LST. The increase in anthropogenic heat emission under heat waves has been attributed to a contributor to the daytime UHI-heat wave interaction (e.g., Zhao et al. 2018; An et al. 2020; Luo et al. 2023).

Figures 9d, e, and f are the same as Figs. 9a, b, and c except for the monsoon season. Under HW_{mon}, the statistical distribution of daytime UHI intensity does not show an increasing shift (Fig. 9d). The mean daytime UHI intensity under HW_{mon} (0.04 °C) is lower than that under $nonHW_{mon}$

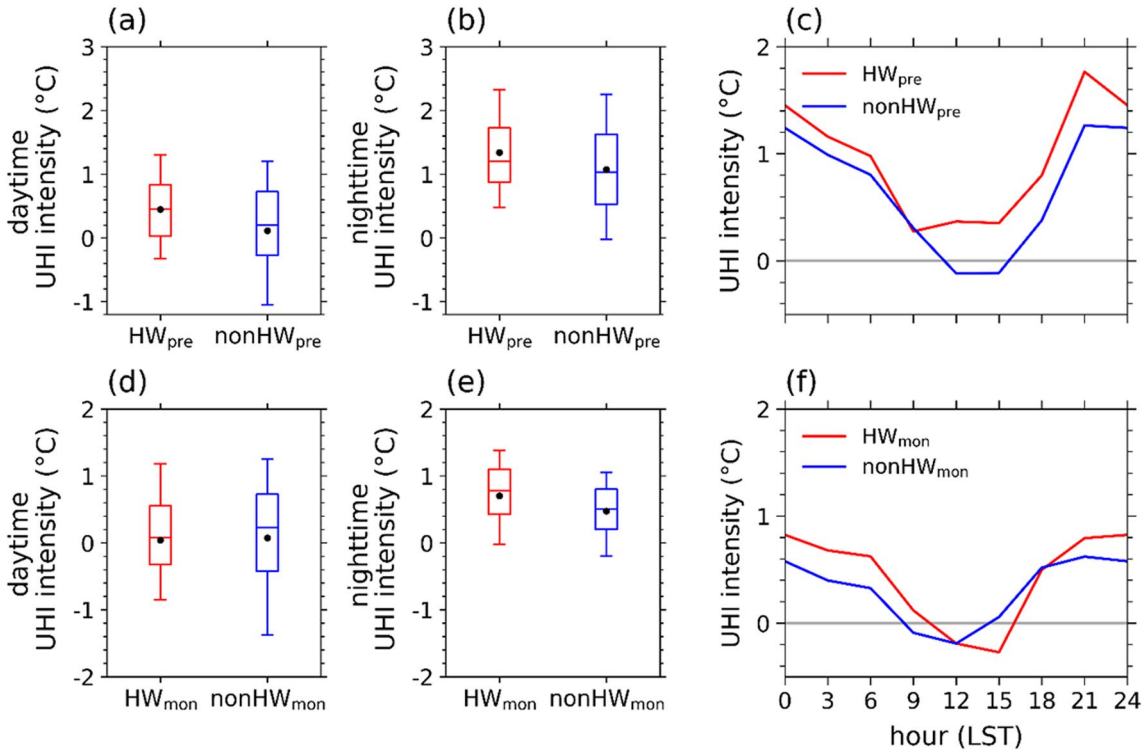

Fig. 9 Box plots of (**a**) daytime and (**b**) nighttime UHI intensities and (**c**) diurnal variations of UHI intensities under heat waves (red) and non-heat waves (blue) in the pre-monsoon season. (**d**, **e**, **f**) Same as (**a**, **b**, **c**) except for the monsoon season. In the box plots, the black dot and horizontal line in each box denote the mean and median, respectively. The upper and lower edges (whiskers) denote the upper quartile (90th percentile) and lower quartile (10th percentile), respectively. The horizontal gray lines in (**c**) and (**f**) indicate zeroes

(non-heat waves in the monsoon season) (0.07 °C), indicating a negative UHI-heat wave interaction. Under HW_{mon}, the 90th percentile (upper quartile) of daytime UHI intensity decreases by 0.05 °C (0.18 °C), while the 10th percentile (lower quartile) increases by 0.52 °C (0.10 °C). Accordingly, the variability of daytime UHI intensity decreases under HW_{mon}. On the other hand, the statistical distribution of nighttime UHI intensity under HW_{mon} shows an increasing shift (Fig. 9e), indicating the synergistic UHI-heat wave interaction. The mean nighttime UHI intensity under HW_{mon} (0.70 °C) is stronger than that under $nonHW_{mon}$ (0.47 °C). The 90th percentile and upper quartile of nighttime UHI intensity increase by 0.34 °C and 0.30 °C under HW_{mon} (1.39 °C and 1.10 °C), while the 10th percentile and lower quartile increase by 0.17 °C and 0.23 °C under HW_{mon} (−0.04 °C and 0.42 °C). Thus, the degree of the synergistic UHI-heat wave interaction in the high percentiles of nighttime UHI intensity is larger than that in the low percentiles of nighttime UHI intensity.

The diurnal variations of UHI intensities under HW_{mon} and $nonHW_{mon}$ also reveal contrasting UHI-heat wave interactions in the daytime and nighttime (Fig. 9f). The UHI intensity in the nighttime under HW_{mon} is stronger than that under $nonHW_{mon}$ by 0.20–0.30 °C. However, the UHI intensity in the daytime except for 0900 LST under HW_{mon} is very similar or weaker than that under $nonHW_{mon}$. At 1500 LST, the UHI intensity under HW_{mon} (−0.27 °C) is weaker by 0.33 °C than that under $nonHW_{mon}$ and has a daily minimum value. The minimum UHI intensity under HW_{mon} is also weaker than the daily minimum UHI intensity under $nonHW_{mon}$ (−0.19 °C) and appears three hours later than that under $nonHW_{mon}$. These characteristics (stronger nighttime UHI intensity, slightly lower daytime UHI intensity, and later occurrence of minimum UHI intensity under heat waves) were also evident in Guangzhou, China under subtropical monsoon climate in summer (Jiang et al. 2019).

Lastly, to get some insights into the UHI-heat wave interaction in relation to meteorological conditions, correlations between UHI intensity and meteorological variables are calculated. Note that all correlation coefficient values presented below are statistically significant at the 95% confidence level. In the pre-monsoon season, the UHI intensity is negatively correlated with the 10-m wind speed in the daytime/nighttime (correlation coefficient = −0.20/−0.19). Thus, the increase in daytime/nighttime 10-m wind speed (0.16/0.17 m s^{-1}, Table 2) is not favorable for the synergistic UHI-heat wave interaction. The correlation between UHI intensity and relative humidity in the daytime/nighttime is

negative (correlation coefficient = −0.10/−0.41), and the correlation between UHI intensity and cloud fraction in the daytime/nighttime is also negative (correlation coefficient = −0.22/−0.31). Thus, the decreases in daytime/nighttime relative humidity and cloud fraction under HW_{pre} (−3.8/−1.7% and −0.7/−0.3, respectively, Table 2) are favorable for the synergistic UHI-heat wave interaction. In the monsoon season, there are a negative correlation between UHI intensity and relative humidity in the nighttime (correlation coefficient = −0.33) and also a negative correlation between UHI intensity and cloud fraction in the nighttime (correlation coefficient = −0.15). Thus, the decreases in nighttime relative humidity and cloud fraction under HW_{mon} (−1.8% and −1.1, Table 2) are favorable for the synergistic nighttime UHI-heat wave interaction. The correlation coefficient between UHI intensity and wind speed in the daytime is 0.05. It is −0.09 for relative humidity and −0.10 for cloud fraction. These low correlations between UHI intensity and meteorological variables in the daytime are a plausible reason for the insignificant daytime UHI-heat wave interaction despite the significant decreases in daytime relative humidity and cloud fraction under HW_{mon} (−6.6% and −1.2, Table 2).

4 Summary and Conclusions

Using meteorological data and reanalysis data for the period of 1995–2019, this study examines the characteristics of the UHI in Dhaka and its interaction with heat waves. Dhaka has experienced an increasing trend of the UHI intensity over the 25 years (0.21 °C per decade). The average UHI intensity is 0.48 °C and the average daily maximum UHI intensity is 2.15 °C. The UHI is strongest in winter and weakest in the monsoon season. In all seasons, the UHI is strongest at 2100 LST and a weak daytime cool island appears. A multiple linear regression analysis is performed to examine the relative importance of the variables that affect the daily maximum UHI intensity. The selected four variables are previous-day daily maximum UHI intensity (PER), wind speed (WS), relative humidity (RH), and cloud fraction (CF). In all seasons, PER (RH) is positively (negatively) correlated with the daily maximum UHI intensity. In the pre-monsoon season, RH is the most important variable and PER is the second most important one. In the monsoon season, RH is the predominantly more important variable than PER, WS, and CF. In the post-monsoon season and winter, PER is the most important variable and RH is the second most important one.

The occurrence frequency of heat waves in Dhaka shows a statistically significant increasing trend in the monsoon season, with its increasing rate of 5.8 days per decade. The analysis of synoptic patterns reveals that under heat waves, anomaly patterns in the pre-monsoon season is distinct from those in the monsoon season. In the pre-monsoon season, heat waves in Bangladesh are associated with mid-to-upper tropospheric anticyclonic-flow and high-pressure anomalies. On the other hand, in the monsoon season, heat waves in Bangladesh are associated with low-to-mid tropospheric anticyclonic-flow and high-pressure anomalies. It is found that under heat waves, the UHI intensity is synergistically intensified in both daytime and nighttime in the pre-monsoon season and in the nighttime only in the monsoon season. The synergistic UHI-heat wave interaction is associated with the decreases in relative humidity and cloud fraction. The synergistic UHI-heat wave interaction occurring in Dhaka could further amplify heat-related risks faced by urban residents. Therefore, when establishing preparedness measures or assessing potential heat-related risks associated with heat waves, it is imperative to take into account the UHI-heat wave interaction.

In this study, through the analysis of available data, we examined the characteristics of the UHI in Dhaka, a city influenced by the South Asian monsoon. Many characteristics are associated with the monsoon climate, for example, weakest UHI in the monsoon season and a strong dependency of the daily maximum UHI intensity on relative humidity, indicating the importance of background climate in UHI characteristics for a city. Bangladesh is the largest deltaic country in the world and vulnerable to climate change. Many major cities in the country including Dhaka have experienced rapid urbanization. To understand and cope with excess urban warming in major cities of Bangladesh, in-depth studies of the UHI and UHI-heat wave interaction for the major cities are needed using all available data. Also, numerical modeling studies that help to understand physical processes behind the UHI and UHI-heat wave interaction are needed.

Acknowledgements The authors are grateful to two anonymous reviewers for providing valuable comments on this work. This work was supported by the National Research Foundation of Korea (NRF) under grant 2021R1A2C1007044.

Funding Open Access funding enabled and organized by Seoul National University.

Data Availability The data at the two meteorological stations were obtained from the Bangladesh Meteorological Department (BMD). The ERA5 data were downloaded from the Copernicus Climate Change Service (C3S) Climate Data Store (CDS).

Declarations

Conflict of Interest The authors declare that they have no conflict of interest.

References

Abrar, R., Sarkar, S.K., Nishtha, K.T., Talukdar, S., Shahfahad Rahman, A., Islam, A.R.M.T., Mosavi, A.: Assessing the spatial mapping of heat vulnerability under urban heat island (UHI) effect in the Dhaka Metropolitan Area. Sustainability **14**, 4945 (2022)

Ahmed, B., Kamruzzaman, M., Zhu, X., Rahman, M.S., Choi, K.: Simulating land cover changes and their impacts on land surface temperature in Dhaka. Bangladesh. Remote Sens. **5**, 5969–5998 (2013)

Ahmed, T., Jin, H.-G., Baik, J.-J.: Spatiotemporal variations of precipitation in Bangladesh revealed by nationwide rain gauge data. Asia-Pac. J. Atmos. Sci. **56**, 593–602 (2020)

Amorim, M.C.C.T.: Daily evolution of urban heat islands in a Brazilian tropical continental climate during dry and rainy periods. Urban Clim. **34**, 100715 (2020)

An, N., Dou, J., González-Cruz, J.E., Bornstein, R.D., Miao, S., Li, L.: An observational case study of synergies between an intense heat wave and the urban heat island in Beijing. J. Appl. Meteorol. Climatol. **59**, 605–620 (2020)

Arifwidodo, S.D., Tanaka, T.: The characteristics of urban heat island in Bangkok, Thailand. Procedia Soc. Behav. Sci. **195**, 423–428 (2015)

Basara, J.B., Hall, P.K., Jr., Schroeder, A.J., Illston, B.G., Nemunaitis, K.L.: Diurnal cycle of the Oklahoma City urban heat island. J. Geophys. Res. Atmos. **113**, D20109 (2008)

BBS: Population and housing census: preliminary report. Bangladesh Bureau of Statistics, Dhaka (2022)

Beck, H.E., Zimmermann, N.E., McVicar, T.R., Vergopolan, N., Berg, A., Wood, E.F.: Present and future Köppen-Geiger climate classification maps at 1-km resolution. Sci. Data **5**, 180214 (2018)

Camilloni, I., Barrucand, M.: Temporal variability of the Buenos Aires, Argentina, urban heat island. Theor. Appl. Climatol. **107**, 47–58 (2012)

Cao, D., Xu, K., Huang, Q.-L., Tam, C.-Y., Chen, S., He, Z., Wang, W.: Exceptionally prolonged extreme heat waves over South China in early summer 2020: the role of warming in the tropical Indian Ocean. Atmos. Res. **278**, 106335 (2022)

Cha, Y., Choi, J., Kim, E.-S., Ahn, J.-B.: Occurrence of heatwave in Korea by the displacement of South Asian high. Clim. Dyn. **58**, 1699–1718 (2022)

Chow, W.T.L., Roth, M.: Temporal dynamics of the urban heat island of Singapore. Int. J. Climatol. **26**, 2243–2260 (2006)

Cui, Y.Y., de Foy, B.: Seasonal variations of the urban heat island at the surface and the near-surface and reductions due to urban vegetation in Mexico City. J. Appl. Meteorol. Climatol. **51**, 855–868 (2012)

Dewan, A., Kiselev, G., Botje, D., Mahmud, G.I., Bhuian, M.H., Hassan, Q.K.: Surface urban heat island intensity in five major cities of Bangladesh: patterns, drivers and trends. Sust. Cities Soc. **71**, 102926 (2021a)

Dewan, A., Kiselev, G., Botje, D.: Diurnal and seasonal trends and associated determinants of surface urban heat islands in large Bangladesh cities. Appl. Geogr. **135**, 102533 (2021b)

Du, H., Wang, D., Wang, Y., Zhao, X., Qin, F., Jiang, H., Cai, Y.: Influences of land cover types, meteorological conditions, anthropogenic heat and urban area on surface urban heat island in the Yangtze River Delta Urban Agglomeration. Sci. Total. Environ. **571**, 461–470 (2016)

Engdaw, M.M., Ballinger, A.P., Hegerl, G.C., Steiner, A.K.: Changes in temperature and heat waves over Africa using observational and reanalysis data sets. Int. J. Climatol. **42**, 1165–1180 (2022)

Erlat, E., Türkeş, M., Aydin-Kandemir, F.: Observed changes and trends in heatwave characteristics in Turkey since 1950. Theor. Appl. Climatol. **145**, 137–157 (2021)

Founda, D., Santamouris, M.: Synergies between Urban Heat Island and Heat Waves in Athens (Greece), during an extremely hot summer (2012). Sci. Rep. **7**, 10973 (2017)

Founda, D., Pierros, F., Petrakis, M., Zerefos, C.: Interdecadal variations and trends of the Urban Heat Island in Athens (Greece) and its response to heat waves. Atmos. Res. **161–162**, 1–13 (2015)

Ganbat, G., Han, J.-Y., Ryu, Y.-H., Baik, J.-J.: Characteristics of the urban heat island in a high-altitude metropolitan city, Ulaanbaatar, Mongolia. Asia-Pac. J. Atmos. Sci. **49**, 535–541 (2013)

Gazi, M.Y., Rahman, M.Z., Uddin, M.M., Rahman, F.M.A.: Spatio-temporal dynamic land cover changes and their impacts on the urban thermal environment in the Chittagong metropolitan area, Bangladesh. GeoJournal **86**, 2119–2134 (2021)

Harun, Z., Reda, E., Abdulrazzaq, A., Abbas, A.A., Yusup, Y., Zaki, S.A.: Urban heat island in the modern tropical Kuala Lumpur: comparative weight of the different parameters. Alex. Eng. J. **59**, 4475–4489 (2020)

He, B.-J.: Potentials of meteorological characteristics and synoptic conditions to mitigate urban heat island effects. Urban Clim. **24**, 26–33 (2018)

Hersbach, H., Bell, B., Berrisford, P., Hirahara, S., Horányi, A., Muñoz-Sabater, J., Nicolas, J., Peubey, C., Radu, R., Schepers, D., Simmons, A., Soci, C., Abdalla, S., Abellan, X., Balsamo, G., Bechtold, P., Biavati, G., Bidlot, J., Bonavita, M., De Chiara, G., Dahlgren, P., Dee, D., Diamantakis, M., Dragani, R., Flemming, J., Forbes, R., Fuentes, M., Geer, A., Haimberger, L., Healy, S., Hogan, R.J., Hólm, E., Janisková, M., Keeley, S., Laloyaux, P., Lopez, P., Lupu, C., Radnoti, G., de Rosnay, P., Rozum, I., Vamborg, F., Villaume, S., Thépaut, J.-N.: The ERA5 global reanalysis. Q. J. R. Meteorol. Soc. **146**, 1999–2049 (2020)

Imran, H.M., Hossain, A., Islam, A.K.M.S., Rahman, A., Bhuiyan, M.A.E., Paul, S., Alam, A.: Impact of land cover changes on land surface temperature and human thermal comfort in Dhaka city of Bangladesh. Earth Syst. Environ. **5**, 667–693 (2021)

Ishtiaque, T.A., Tasin, Z.T., Akter, K.S.: Urban heat island intensity assessment through comparative study on land surface temperature and normalized difference vegetation index: a case study of Chittagong, Bangladesh. Int. J. Urban Civ. Eng. **11**, 37–42 (2017)

Islam, M.D., Chakraborty, T., Alam, M.S., Islam, K.S.: Urban heat island effect analysis using integrated geospatial techniques: a case study on Khulna city, Bangladesh. In: International Conference on Climate Change (ICCC-2019), Dhaka, Bangladesh (2019)

Islam, M.S., Islam, K.S.: Application of thermal infrared remote sensing to explore the relationship between land use-land cover changes and urban heat island effect: a case study of Khulna city. J. Bangladesh Inst. Plan. **6**, 49–60 (2013)

Jiang, S., Lee, X., Wang, J., Wang, K.: Amplified urban heat islands during heat wave periods. J. Geophys. Res. Atmos. **124**, 7797–7812 (2019)

Jiang, J., Liu, Y., Mao, J., Wu, G.: Extreme heatwave over Eastern China in summer 2022: the role of three oceans and local soil moisture feedback. Environ. Res. Lett. **18**, 044025 (2023)

Jongtanom, Y., Kositanont, C., Baulert, S.: Temporal variations of urban heat island intensity in three major cities, Thailand. Mod. Appl. Sci. **5**, 105–110 (2011)

Kamma, J., Manomaiphiboon, K., Aman, N., Thongkamdee, T., Chuangchote, S., Bonnet, S.: Urban heat island analysis for Bangkok:

multi-scale temporal variation, associated factors, directional dependence, and cool island condition. ScienceAsia **46**, 213–223 (2020)
Khatun, M., Khatun, R., Hossen, M.S.: Urban heat island characteristics under different land use land covers in Dhaka, Bangladesh. Int. J. Curr. Res. **12**, 9627–9635 (2020)
Kim, Y.-H., Baik, J.-J.: Maximum urban heat island intensity in Seoul. J. Appl. Meteorol. **41**, 651–659 (2002)
Kim, Y.-H., Baik, J.-J.: Spatial and temporal structure of the urban heat island in Seoul. J. Appl. Meteorol. **44**, 591–605 (2005)
Kim, M., Lee, K., Cho, G.-H.: Temporal and spatial variability of urban heat island by geographical location: a case study of Ulsan, Korea. Build. Environ. **126**, 471–482 (2017)
Kong, J., Zhao, Y., Carmeliet, J., Lei, C.: Urban heat island and its interaction with heatwaves: a review of studies on mesoscale. Sustainability **13**, 10923 (2021)
Kotharkar, R., Bagade, A., Ramesh, A.: Assessing urban drivers of canopy layer urban heat island: a numerical modeling approach. Landsc. Urban Plan. **190**, 103586 (2019)
Kottek, M., Grieser, J., Beck, C., Rudolf, B., Rubel, F.: World map of the Köppen-Geiger climate classification updated. Meteorol. Z. **15**, 259–263 (2006)
Kumar, R., Mishra, V.: Decline in surface urban heat island intensity in India during heatwaves. Environ. Res. Commun. **1**, 031001 (2019)
Kumar, A., Mukherjee, M., Goswami, A.: Inter-seasonal characterization and correlation of Surface Urban Heat Island (SUHI) and Canopy Urban Heat Island (CUHI) in the urbanized environment of Delhi. Remote Sens. Appl. Soc. Environ. **30**, 100970 (2023)
Lee, S.-H., Baik, J.-J.: Statistical and dynamical characteristics of the urban heat island intensity in Seoul. Theor. Appl. Climatol. **100**, 227–237 (2010)
Leya, R.S., Jodder, P.K., Rahaman, K.R., Chowdhury, M.A., Parida, D., Islam, M.S.: Spatial variations of urban heat island development in Khulna city, Bangladesh: implications for urban planning and development. Earth Syst. Environ. **6**, 865–884 (2022)
Li, D., Bou-Zeid, E.: Synergistic interactions between urban heat islands and heat waves: the impact in cities is larger than the sum of its parts. J. Appl. Meteorol. Climatol. **52**, 2051–2064 (2013)
Li, G., Zhang, X., Mirzaei, P.A., Zhang, J., Zhao, Z.: Urban heat island effect of a typical valley city in China: responds to the global warming and rapid urbanization. Sust. Cities Soc. **38**, 736–745 (2018)
Lin, X.-C., Yu, S.-Q.: Interdecadal changes of temperature in the Beijing region and its heat island effect. Chin. J. Geophys. **48**, 47–54 (2005)
Liu, W., Ji, C., Zhong, J., Jiang, X., Zheng, Z.: Temporal characteristics of the Beijing urban heat island. Theor. Appl. Climatol. **87**, 213–221 (2007)
Luo, F., Yang, Y., Zong, L., Bi, X.: The interactions between urban heat island and heat waves amplify urban warming in Guangzhou, China: roles of urban ventilation and local climate zones. Front. Environ. Sci. **11**, 1084473 (2023)
Manoli, G., Fatichi, S., Schläpfer, M., Yu, K., Crowther, T.W., Meili, N., Burlando, P., Katul, G.G., Bou-Zeid, E.: Magnitude of urban heat islands largely explained by climate and population. Nature **573**, 55–60 (2019)
Memon, R.A., Leung, D.Y.C., Liu, C.-H.: An investigation of urban heat island intensity (UHII) as an indicator of urban heating. Atmos. Res. **94**, 491–500 (2009)
Morris, C.J.G., Simmonds, I., Plummer, N.: Quantification of the influences of wind and cloud on the nocturnal urban heat island of a large city. J. Appl. Meteorol. **40**, 169–182 (2001)
Nissan, H., Burkart, K., de Perez, E.C., Van Aalst, M., Mason, S.: Defining and predicting heat waves in Bangladesh. J. Appl. Meteorol. Climatol. **56**, 2653–2670 (2017)
Oke, T.R., Mills, G., Christen, A., Voogt, J.A.: Urban climates. Cambridge University Press, Cambridge (2017)
Ortiz, L.E., Gonzalez, J.E., Wu, W., Schoonen, M., Tongue, J., Bornstein, R.: New York City impacts on a regional heat wave. J. Appl. Meteorol. Climatol. **57**, 837–851 (2018)
Ouchra, H., Belangour, A., Erraissi, A.: Machine learning algorithms for satellite image classification using Google Earth Engine and Landsat satellite data: Morocco case study. IEEE Access **11**, 71127–71142 (2023)
Panda, D.K., AghaKouchak, A., Ambast, S.K.: Increasing heat waves and warm spells in India, observed from a multiaspect framework. J. Geophys. Res. Atmos. **122**, 3837–3858 (2017)
Park, K., Jin, H.-G., Baik, J.-J.: Contrasting interactions between urban heat islands and heat waves in Seoul, South Korea, and their associations with synoptic patterns. Urban Clim. **49**, 101524 (2023)
Parvin, N.S., Abudu, D.: Estimating urban heat island intensity using remote sensing techniques in Dhaka city. Int. J. Sci. Eng. Res. **8**, 289–298 (2017)
Peel, M.C., Finlayson, B.L., McMahon, T.A.: Updated world map of the Köppen-Geiger climate classification. Hydrol. Earth Syst. Sci. **11**, 1633–1644 (2007)
Perkins, S.E.: A review on the scientific understanding of heatwaves–their measurement, driving mechanisms, and changes at the global scale. Atmos. Res. **164–165**, 242–267 (2015)
Qian, Y., Chakraborty, T.C., Li, J., Li, D., He, C., Sarangi, C., Chen, F., Yang, X., Leung, L.R.: Urbanization impact on regional climate and extreme weather: current understanding, uncertainties, and future research directions. Adv. Atmos. Sci. **39**, 819–860 (2022)
Rahman, M.N., Rony, M.R.H., Jannat, F.A., Pal, S.C., Islam, M.S., Alam, E., Islam, A.R.M.T.: Impact of urbanization on urban heat island intensity in major districts of Bangladesh using remote sensing and geo-spatial tools. Climate **10**, 3 (2022)
Ramakreshnan, L., Aghamohammadi, N., Fong, C.S., Ghaffarianhoseini, A., Wong, L.P., Sulaiman, N.M.: Empirical study on temporal variations of canopy-level Urban Heat Island effect in the tropical city of Greater Kuala Lumpur. Sust. Cities Soc. **44**, 748–762 (2019)
Ramamurthy, P., Bou-Zeid, E.: Heatwaves and urban heat islands: a comparative analysis of multiple cities. J. Geophys. Res. Atmos. **122**, 168–178 (2017)
Rashid, N., Alam, J.A.M.M., Chowdhury, M.A., Islam, S.L.U.: Impact of landuse change and urbanization on urban heat island effect in Narayanganj city, Bangladesh: a remote sensing-based estimation. Environ. Chall. **8**, 100571 (2022)
Rizvi, S.H., Alam, K., Iqbal, M.J.: Spatio-temporal variations in urban heat island and its interaction with heat wave. J. Atmos. Sol.-Terr. Phys. **185**, 50–57 (2019)
Roy, D.P., Wulder, M.A., Loveland, T.R., Woodcock, C.E., Allen, R.G., Anderson, M.C., Helder, D., Irons, J.R., Johnson, D.M., Kennedy, R., Scambos, T.A., Schaaf, C.B., Schott, J.R., Sheng, Y., Vermote, E.F., Belward, A.S., Bindschadler, R., Cohen, W.B., Gao, F., Hipple, J.D., Hostert, P., Huntington, J., Justice, C.O., Kilic, A., Kovalskyy, V., Lee, Z.P., Lymburner, L., Masek, J.G., McCorkel, J., Shuai, Y., Trezza, R., Vogelmann, J., Wynne, R.H., Zhu, Z.: Landsat-8: science and product vision for terrestrial global change research. Remote Sens. Environ. **145**, 154–172 (2014)
Roy, S., Pandit, S., Eva, E.A., Bagmar, M.S.H., Papia, M., Banik, L., Dube, T., Rahman, F., Razi, M.A.: Examining the nexus between land surface temperature and urban growth in Chattogram Metropolitan Area of Bangladesh using long term Landsat series data. Urban Clim. **32**, 100593 (2020)
Ryu, Y.-H., Baik, J.-J.: Quantitative analysis of factors contributing to urban heat island intensity. J. Appl. Meteorol. Climatol. **51**, 842–854 (2012)

Santamouris, M.: Analyzing the heat island magnitude and characteristics in one hundred Asian and Australian cities and regions. Sci. Total. Environ. **512–513**, 582–598 (2015)

Schatz, J., Kucharik, C.J.: Seasonality of the urban heat island effect in Madison, Wisconsin. J. Appl. Meteorol. Climatol. **53**, 2371–2386 (2014)

Shourav, M.S.A., Shahid, S., Singh, B., Mohsenipour, M., Chung, E.-S., Wang, X.-J.: Potential impact of climate change on residential energy consumption in Dhaka city. Environ. Model. Assess. **23**, 131–140 (2018)

Theeuwes, N.E., Steeneveld, G.-J., Ronda, R.J., Rotach, M.W., Holtslag, A.A.M.: Cool city mornings by urban heat. Environ. Res. Lett. **10**, 114022 (2015)

Thomas, G., Sherin, A.P., Ansar, S., Zachariah, E.J.: Analysis of urban heat island in Kochi, India, using a modified local climate zone classification. Procedia Environ. Sci. **21**, 3–13 (2014)

Todhunter, P.E.: Environmental indices for the Twin Cities Metropolitan Area (Minnesota, USA) urban heat island – 1989. Clim. Res. **6**, 59–69 (1996)

Tzavali, A., Paravantis, J.P., Mihalakakou, G., Fotiadi, A., Stigka, E.: Urban heat island intensity: a literature review. Fresenius Environ. Bull. **24**, 4537–4554 (2015)

Uddin, A.S.M.S., Khan, N., Islam, A.R.M.T., Kamruzzaman, M., Shahid, S.: Changes in urbanization and urban heat island effect in Dhaka city. Theor. Appl. Climatol. **147**, 891–907 (2022)

Varentsov, M.I., Konstantinov, P.I., Shartova, N.V., Samsonov, T.E., Kargashin, P.E., Varentsov, A.I., Fenner, D., Meier, F.: Urban heat island of the Moscow megacity: the long-term trends and new approaches for monitoring and research based on crowdsourcing data. IOP Conf. Ser. Earth Environ. Sci. **606**, 012063 (2020)

Vogel, J., Afshari, A.: Comparison of urban heat island intensity estimation methods using urbanized WRF in Berlin, Germany. Atmosphere **11**, 1338 (2020)

Wang, W., Zhou, W., Ng, E.Y.Y., Xu, Y.: Urban heat islands in Hong Kong: statistical modeling and trend detection. Nat. Hazards **83**, 885–907 (2016)

Wang, A., Li, X.-X., Xin, R., Chew, L.W.: Impact of anthropogenic heat on urban environment: a case study of Singapore with high-resolution gridded data. Atmosphere **14**, 1499 (2023)

Yang, P., Ren, G., Liu, W.: Spatial and temporal characteristics of Beijing urban heat island intensity. J. Appl. Meteorol. Climatol. **52**, 1803–1816 (2013)

Yao, R., Wang, L., Huang, X., Liu, Y., Niu, Z., Wang, S., Wang, L.: Long-term trends of surface and canopy layer urban heat island intensity in 272 cities in the mainland of China. Sci. Total Environ. **772**, 145607 (2021)

Zahid, M., Rasul, G.: Changing trends of thermal extremes in Pakistan. Clim. Change **113**, 883–896 (2012)

Zhang, R., Sun, C., Zhu, J., Zhang, R., Li, W.: Increased European heat waves in recent decades in response to shrinking Arctic sea ice and Eurasian snow cover. npj Clim. Atmos. Sci. **3**, 7 (2020)

Zhang, Z., Paschalis, A., Mijic, A., Meili, N., Manoli, G., van Reeuwijk, M., Fatichi, S.: A mechanistic assessment of urban heat island intensities and drivers across climates. Urban Clim. **44**, 101215 (2022)

Zhao, L., Lee, X., Smith, R.B., Oleson, K.: Strong contributions of local background climate to urban heat islands. Nature **511**, 216–219 (2014)

Zhao, L., Oppenheimer, M., Zhu, Q., Baldwin, J.W., Ebi, K.L., Bou-Zeid, E., Guan, K., Liu, X.: Interactions between urban heat islands and heat waves. Environ. Res. Lett. **13**, 034003 (2018)